International Journal of Robotics and Automation, Vol. 27, No. 1, 2012

DESIGN AND ANALYSIS OF AN ACTIVE BALL-HANDLING MECHANISM FOR SOCCER ROBOT IN ROBOCUP

Aolin Tang,* Qixin Cao,* and Chunshan Xu**

Abstract

Dribbling ability is of great value to a soccer robot in the RoboCup Middle Size League (MSL). In the past, most soccer robots equipped passive ball-handling mechanism because of its simplicity. But it can only provide a quite limited control over the ball, while active ball-handling mechanism could improve the robot's dribbling ability significantly. In this paper, an active ball-handling mechanism is designed and utilized in the Jiaolong soccer robot. The ball-handling mechanism consists of two friction wheels driven by DC motors and the ball-handling process is performed by individual control of two DC motors' rotation velocities. In the first part of the paper, theoretical model of the active ball-handing mechanism is derived and effects caused by different ways of installation and different installation parameters are analyzed, which can help us design the ball-handling mechanism. After that, control system of active ball-handling is introduced. A velocity coordinator is devised to optimize the motion of robot. In addition, a position loop is added to prevent the ball from losing: based on the ball's position obtained from the omni-directional vision system, a fuzzy controller is equipped to adjust velocities of two DC motors, so as to make sure the ball is always under control. The result of experiments show that it works as expected.

Key Words

Active ball-handling, soccer robot, RoboCup, velocity coordinator, fuzzy control

1. Introduction

RoboCup [1] is an international project that promotes AI, robotics and related fields. The ultimate goal of the RoboCup project is to develop a team of fully autonomous humanoid robots that can win against the human world champion team in soccer by 2050. Middle Size Robot League is an important part of RoboCup. During the match of Middle Size Robot League, a soccer robot needs to search the ball, grab the ball, dribble and shoot. The ability of grabbing and handling the ball is essential to a soccer robot. With good ball-handling ability, the robot can shake off defenders and create opportunities to goal. In the past, passive ball-handling mechanism was massively implemented in the Middle Size Robot League of RoboCup [2]. The principal of passive ball-handling mechanism is very simple, for example, a small fork or a clamp, shaped to fit around the ball. But the size of fork or clamp is limited by the rule of "ball holding". During a game, the ball must not entering the convex hull of a robot by more than a third of its diameter except when the robot is stopping the ball or not entering the convex hull of a robot by more than half of its diameter if the robot is stopping the ball [1]. When the robot is accelerating, passive ball-handling mechanism can push the ball forwards. But when the robot is decelerating, the ball's momentum carries it away from the robot. That is because in such a system, the force can only be exerted on the ball with a pointing away direction from the robot. So to slow down or move sideways, the robot has to rotate around the vertical axis of the ball, which brings extra limitation to the trajectory planning. To solve this problem, active ball-handling mechanism was introduced into RoboCup [30]. With an active ball-handling mechanism, the robot can move around easily and freely with the ball under control. The ball is kept in the same rhythm of the robot. The robot can finish more complicated movement to break through, such as the famous "Marseille turn" of Zidane. With improved ball-handling ability, more tactical cooperation like wall pass can also be carried out during the match.

In the Small Size Robot League, active ball-handling mechanism was utilized as early as in the RoboCup 2000 [2]. The team Cornell introduced a lot of innovation of active ball-handling mechanism in that period [3]. With that, Cornell dominated the Small Size Robot League in that year. Some teams in the Middle Size Robot League also

* State Key Lab of Mechanical Systems and Vibration, Shanghai Jiao Tong University, PR China; e-mail: altang1988@gmail.com, qxcao@sjtu.edu.cn

** Shanghai Ingenious Automation Technology Co., Ltd, PR China; e-mail: xcs2004@263.net

Recommended by Prof. H. Hagras

(DOI: 10.2316/Journal.206.2012.1.206-3619)

adopted this method [4]. The active ball-handling mechanism of Cornell was a rotating bar with a latex cover placed just above the kicking mechanism. Upon contact with the ball, the rotation of the bar imparted a backward spin on the ball [3]. But one disadvantage of this mechanism is that the tangential velocity of the ball is uncontrollable. Later, new kinds of active ball-handling mechanism were designed and utilized, such as the active ball-handling mechanism of Cambada (the champion of RoboCup2008) [5], which uses only one friction wheel, the active ball-handling mechanism of FU fighter [6], Eindhoven University of Technology (the runner-up of RoboCup2009) [7], ENDEAVOR (the champion of RoboCup China 2010) [8], NuBot (the champion of RoboCup China 2008) [9] and Team Water [10], which consists of two friction wheels driven by DC motors (Omni wheels [6] or rubber wheels [7], [8], [9], [10]). There are also different ways to install the friction wheels. The effect caused by different installations will be discussed in detail later. Touch-sensitive ball-handling mechanism is also studied. In [11] and [12], four sensors are implemented to enable the robot have force and position feedback with respect to the ball. In [19], a combination of a capacitive and a pressure sensor is used to obtain the accurate information of the ball position and movement within the ball handling device. However, no further results have been presented yet. At present, a lot of control algorithms for active ball-handling have been proposed, such as open loop control system in the early period [3]. In [8], [9], [13], [14], the ball-handling process is performed by individual control of two DC motors' rotation velocities in a close-loop way. But the motion state of the ball is not taken into consideration. Some facts, such as the uncertainty of field condition (the ball may hop around when the field is unsmooth), error of installation, might cause unstable ball-handling process. Before the match, empirical adjustment of the control system is needed to achieve a good result. In [15], [16], the ball-handling mechanism consists of two levers. The rotation of the levers can be obtained using potentiometers. Ball-handling controller is designed to maintain the angle of the lever at a preferred angle, which corresponds to a desired distance between the ball and the robot. But controllers of two levers work independently and the design of the controller is a little complicated.

The goal of this paper is to propose a method for the design and control of an active ball-handling mechanism. In this work, two DC motors are directly controlled to handle the ball according to the velocity of the ball and its direction, which is easy to realize. This method is also used in [8], [9]. But the novelty of this paper is the proposed theoretical model of the active ball-handling mechanism used for control. And effects caused by different kinds of installation are given. In addition, a velocity coordinator is devised to optimize the motion of robot, and a fuzzy controller is equipped in the feedback loop to increase the robustness of the system.

This paper is organized as follows. After the introduction, a theoretical model of the active ball-handling mechanism (composed of two wheels, driven by two DC motors) will be derived in Section 2. And effects caused by different ways of installation or different installation parameters are also given in this section. Based on the model, the control algorithm is designed, as introduced in Section 3. A prototype is designed and manufactured. Experiments in simulation and in practice are both carried out as described in Section 4. Finally, the conclusions will be drawn and future work will be given in Section 5.

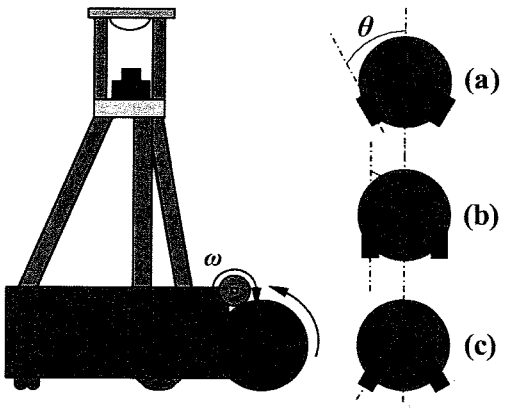

Figure 1. Three different installation styles: (a) toe-out style ($\theta > 0°$ and $\theta < 90°$), (b) parallel style ($\theta = 0°$) and (c) toe-in style ($\theta > 90°$ and $\theta < 180°$).

2. Theoretical Model of the Active Ball-Handling Mechanism

2.1 Different Installation Styles

There are different kinds of active ball-handling mechanism. For example, with one friction wheel, with two friction wheels, bar dribblers or force-feedback handling mechanism. As mentioned before, for bar dribblers and one friction wheel, only longitudinal velocity component of the ball is controllable. Force-feedback handling mechanism is still unpractical. Thus, two friction wheel style is adopted in this paper.

The elementary diagram of the ball-handling mechanism with two friction wheels is schematically depicted in Fig. 1. There are three different installation styles. All of them can realize the rotation of the ball around both the vertical and the horizontal axis, but the ball-handling effects are different. The toe-out style can pull the ball towards the centre of the ball-handling mechanism automatically. Ball approaching in a big range of direction can be taken under control easily rather than rebounded. But the contact area between the friction wheels and the ball is smaller than other two styles, which means the force exerted on the ball is smaller, which is disadvantageous to the robot when grabbing the ball with opponents. For the toe-in style, the contact area is larger. The force exerted on the ball can be greater. But it is hard to take the ball approaching from the side under control since the toe-in style cannot pull the ball to the centre of the ball-handling mechanism automatically. The parallel style falls somewhere in between. In this paper, the toe-out style is chosen.

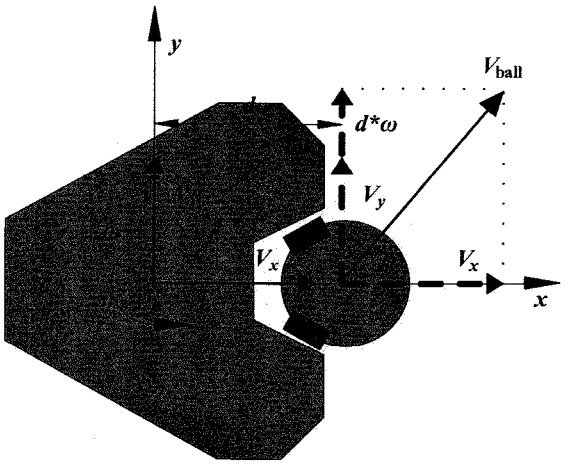

Figure 2. Relation between the velocity of the robot and the velocity of the ball.

2.2 Kinematic Model

In this section, a theoretical model of the active ball-handling mechanism will be derived. First of all, we assign a coordinate system on the soccer robot, as depicted in Fig. 2.

The positive direction of X axis points towards right ahead of the robot, and the positive direction of Y axis towards left. Anticlockwise angle is positive when viewed from above. The definitions of symbols in Fig. 2 are as follows:

- V_x, V_y and ω denote the x, y and angular components of the velocity of the robot.
- The distance between the centre of the ball and the centre of the robot is called d.
- V_{ball} indicates the resulting velocity of the ball at an angle of φ.

From Fig. 2, it is easy to calculate the velocity of the ball and its direction from the velocity and the angular velocity of the robot:

$$V_{ball} = V_x \cdot \vec{e}_x + (V_y + \omega \cdot d) \cdot \vec{e}_y \tag{1}$$

$$\varphi = \arctan \frac{V_y + \omega \cdot d}{V_x} \tag{2}$$

The ball is directly driven by two wheels. To handle the ball, we need to find out the relation between the velocity of the ball and angular velocities of two friction wheels. Two wheels are placed on the top half of the ball and $1/3 \times d_{ball}$ away from the endpoint of the ball to avoid ball holding, as shown in Fig. 3. The ball enters the convex hull of the robot for one-third of its diameter, which is the maximum allowed by the rules as mentioned before. When the direction of ball's velocity $\varphi \in [360° - \theta, \theta]$, the relation between the ball's velocity and two wheels' angular velocities are illustrated in Fig. 3. Here the rotation of the ball around Z axis will not be taken into consideration. That is because the rotation around Z axis is independent with the movement in the plane of XOY.

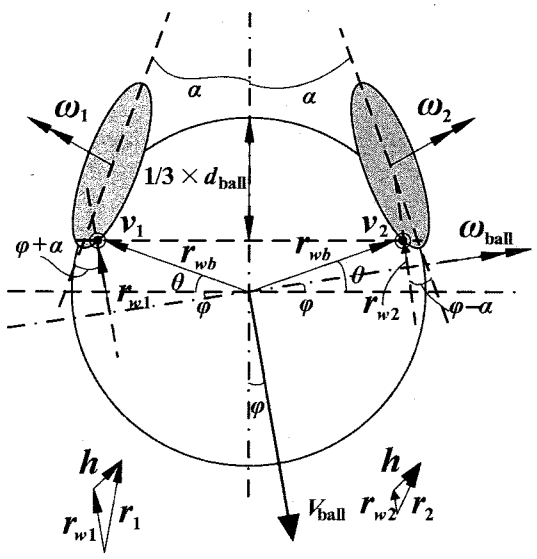

Figure 3. Relation between the velocity of the ball (V_{ball}) and angular velocities of two wheels (ω_1, ω_2) when $\varphi \in [360° - \theta, \theta]$.

The definitions of symbols in Fig. 3 are given as:

- V_{ball} indicates the resulting velocity of the ball at an angle φ.
- V_1 and V_2 donate velocities of two contact points, respectively.
- ω_1 and ω_2 are angular velocities of two friction wheels.
- ω_{ball} stands for the angular velocity of the ball around its axis of rotation.
- d_{ball} is the diameter of the ball, while r_{ball} is the radius of the ball.
- r_{wheel} is the radius of the friction wheel. α is the angle between the plane of wheel and X axis.
- r_1 and r_2 are distances from the ball's axis of rotation to two contact points.
- r_{w1} and r_{w2} are auxiliary radii for calculation. r_{w1} is the projection of r_1 on the horizontal plane and r_{w2} is the horizontal projection of r_2. r_{wb} is also an auxiliary radius for calculation. It indicates the horizontal projection of the radius which is through the contact point.
- h is the distance from the contact point to the XOY plane.

Using the schematic representation of relevant velocities, radii and angles shown in Fig. 3, the relation between the ball's velocity and two wheels' angular velocities can be obtained. The ball is driven to rotate with an angular velocity of ω_{ball}. The centre of the ball moves with a velocity of V_{ball} at angle φ. We have:

$$V_{ball} = \omega_{ball} \cdot r_{\text{ball}} \tag{3}$$

When no slip occurs along the direction of V_1 and V_2, the velocity of the contact point on the ball can be obtained,

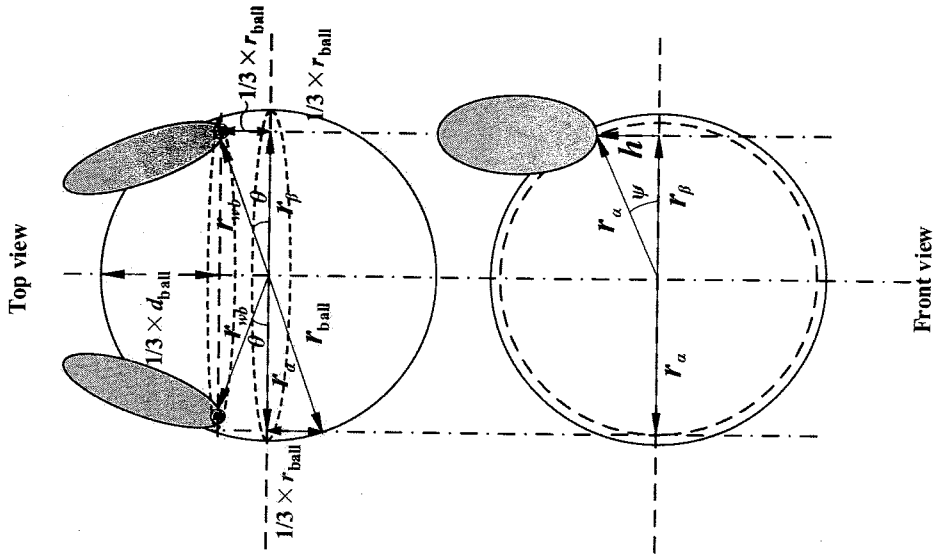

Figure 4. The top view and the front view of the active ball-handling mechanism.

and it should equal the velocity of the contact point on the wheel along the direction of V_1 or V_2. Thus:

$$V_1 = \omega_{ball} \cdot r_1 = \omega_1 \cdot r_{wheel} \cdot \cos(\alpha + \varphi) \tag{4}$$

$$V_2 = -\omega_{ball} \cdot r_2 = -\omega_2 \cdot r_{wheel} \cdot \cos(\varphi - \alpha) \tag{5}$$

In (4) and (5), α, r_{wheel} and r_{ball} can be obtained by measuring. ω_{ball} can be calculated using (3). But r_1 and r_2 are still unknown. From Fig. 3 we can see that r_{w1} and r_{w2} are perpendicular to the height h. Based on the Pythagorean Theorem, it is easy to obtain:

$$r_1 = \sqrt{r_{w1}^2 + h^2} \tag{6}$$

$$r_2 = \sqrt{r_{w2}^2 + h^2} \tag{7}$$

In (6) and (7), r_{w1} and r_{w2} could be obtained by:

$$r_{w2} = r_{wb} \cdot \sin(\theta - \varphi) \tag{8}$$

$$r_{w1} = r_{wb} \cdot \sin(\varphi + \theta) \tag{9}$$

Substituting (6)–(9) into (4) and (5):

$$\omega_1 = \frac{V_{ball} \cdot \sqrt{(r_{wb}\sin(\theta - \varphi))^2 + h^2}}{r_{ball} \cdot r_{wheel} \cdot \cos(\alpha + \varphi)} \tag{10}$$

$$\omega_2 = -\frac{V_{ball} \cdot \sqrt{(r_{wb}\sin(\varphi + \theta))^2 + h^2}}{r_{ball} \cdot r_{wheel} \cdot \cos(\varphi - \alpha)} \tag{11}$$

In (10) and (11), r_{wb}, θ and h are still needed to get angular velocities of two friction wheels ω_1 and ω_2. We can calculate r_{wb}, angle θ and height h with the help of Fig. 4. Figure 4 is the top view and the front view of the active ball-handling mechanism. The definitions of symbols in Fig. 4 are as follows:

- d_{ball} is the diameter of the ball, while r_{ball} is the radius of the ball.
- h is the distance from the contact point to the XOY plane.
- r_{wb} is an auxiliary radius for calculation, which indicates the horizontal projection of the radius through the contact point. θ is the angel between r_{wb} and Y axis. r_α r_β are also auxiliary radii for calculation. r_α donates the radius of the circle which is $1/3 \times d_{ball}$ away from the endpoint of the ball. r_β is the projection of the radius r_{wb} on the plain which is $1/3 \times d_{ball}$ away from the endpoint of the ball.
- Ψ is the angle between r_α and r_β.

Since r_α donates the radius of the circle $1/3 \times d_{ball}$ away from the endpoint of the ball. r_α can be calculated by:

$$r_\alpha = \sqrt{r_{ball}^2 - (r_{ball}/3)^2} = \sqrt{\frac{8}{9}} r_{ball} \tag{12}$$

And from the front view in Fig. 4, we get:

$$r_\beta = r_\alpha \cdot \cos\psi \tag{13}$$

$$h = r_\alpha \cdot \sin\psi \tag{14}$$

From the top view:

$$r_{wb} = \sqrt{r_\beta^2 + \left(\frac{1}{3} r_{ball}\right)^2} \tag{15}$$

$$\theta = \arctan\frac{r_{ball}}{3r_\beta} \tag{16}$$

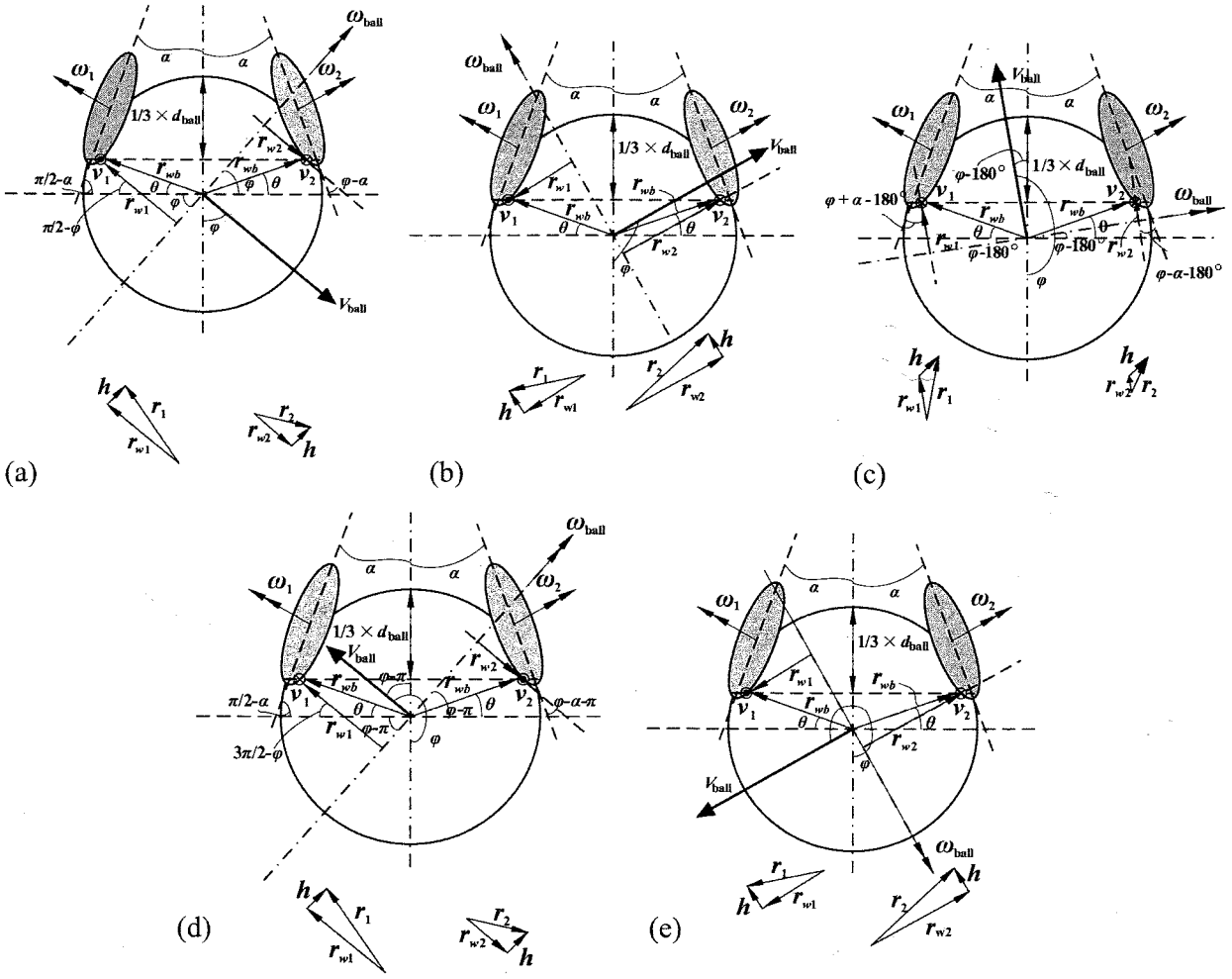

Figure 5. Relation between the velocity of the ball and angular velocities of two wheels when: (a) $\varphi \in [\theta,\ 90^\circ + \theta]$; (b) $\varphi \in [90^\circ + \theta,\ 180^\circ - \theta]$; (c) $\varphi \in [180^\circ - \theta,\ 180^\circ + \theta]$; (d) $\varphi \in [180^\circ + \theta,\ 270^\circ - \theta]$; (e) $\varphi \in [270^\circ - \theta,\ 360^\circ - \theta]$.

Combining (12) (13) and (16), the relation between Ψ and θ can be derived:

$$\tan\theta = \frac{1}{\sqrt{8}\cos\psi} \tag{17}$$

Substituting (14) (15) (16) into (10) and (11), we have:

$$\omega_1 = \frac{V_{ball}\sqrt{\left(\frac{8}{9}\cos^2\psi + \frac{1}{9}\right)\sin^2(\varphi-\theta) + \frac{8}{9}\sin^2\psi}}{r_{wheel}\cdot\cos(\alpha+\varphi)} \tag{18}$$

$$\omega_2 = -\frac{V_{ball}\sqrt{\left(\frac{8}{9}\cos^2\psi + \frac{1}{9}\right)\sin^2(\varphi+\theta) + \frac{8}{9}\sin^2\psi}}{r_{wheel}\cdot\cos(\varphi-\alpha)} \tag{19}$$

In (18) and (19), Ψ, θ, r_{wheel} and α are determined after installation of the active ball-handling mechanism. ω_1 and ω_2 are only determined by the resultant velocity of the ball V_{ball} and its direction φ.

In other conditions, the same conclusion can also be derived. For example, when $\varphi \in [\theta, 90^\circ + \theta]$, relation between the velocity of the ball and angular velocities of two wheels are illustrated in Fig. 5 (a).

The definitions of symbols in Fig. 5 are the same as in Fig. 3. And relations obtained are almost the same except (4) (5) (8) and (9). In this case, (4) and (5) should be:

$$V_1 = \omega_{ball}\cdot r_1 = \omega_1\cdot r_{wheel}\cdot\cos(\alpha+\varphi) \tag{20}$$

$$V_2 = \omega_{ball}\cdot r_2 = -\omega_2\cdot r_{wheel}\cdot\cos(\varphi-\alpha) \tag{21}$$

And (8) and (9) should be:

$$r_{w2} = r_{wb}\cdot\sin(\varphi-\theta) \tag{22}$$

$$r_{w1} = r_{wb}\cdot\sin(\varphi+\theta) \tag{23}$$

With those new relations, we get:

$$\omega_1 = \frac{V_{ball}\cdot\sqrt{\left(\frac{8}{9}\cos^2\psi + \frac{1}{9}\right)\sin^2(\varphi-\theta) + \frac{8}{9}\sin^2\psi}}{r_{wheel}\cdot\cos(\alpha+\varphi)} \tag{24}$$

$$\omega_2 = -\frac{V_{ball}\cdot\sqrt{\left(\frac{8}{9}\cos^2\psi + \frac{1}{9}\right)\sin^2(\varphi+\theta) + \frac{8}{9}\sin^2\psi}}{r_{wheel}\cdot\cos(\varphi-\alpha)} \tag{25}$$

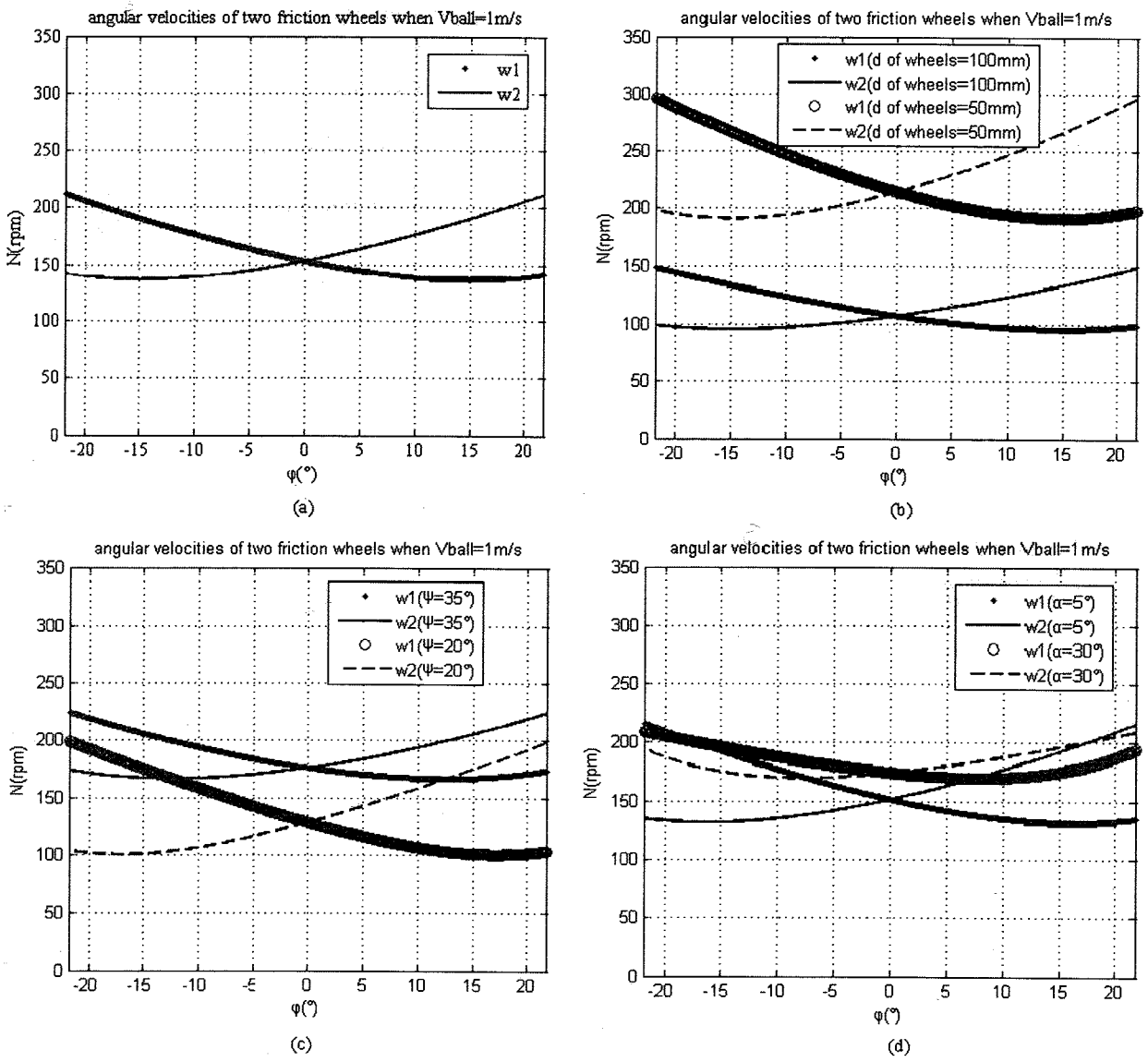

Figure 6. Angular velocities of two DC motors needed ($\omega_1\omega_2$) when the velocity of the ball $V_{ball} = 1$ m/s and its direction φ changes from $-\theta$ ($-21.8°$) to θ ($21.8°$). In (a), $d_{wheel} = 70$ mm, $\alpha = 10°$, $\theta \approx 21.8°$ and $\Psi \approx 27.9°$.

We can find that (24) and (25) are consistent with (18) and (19) because $\sin^2(\varphi - \theta) = \sin^2(\theta - \varphi)$. And in other conditions shown in Fig. 5, (24) and (25) can also be obtained.

2.3 Effects Caused by Installation

Thus using (24) and (25), we can calculate angular velocities of two DC motors needed to drive the ball. When $d_{wheel} = 70$ mm, $\alpha = 10°$, $r_\beta \approx 5/6\, r_{ball}$ and $\theta \approx 21.8°$ (from (17) we can get $\Psi \approx 27.9°$), the velocity of the ball V_{ball} is 1 m/s, and its direction φ varies from $-\theta$ to θ, values of ω_1 and ω_2 are shown in the left figure of Fig. 6(a). To show those changes brought by different parameters clearly, only values of ω_1, ω_2 are depicted here. In fact, ω_2 is negative.

With different parameters (d_{wheel}, Ψ, θ or α), angular velocities of two DC motors needed are different. For example, when the diameter of two friction wheels changed from 70 to 100 or 50 mm, angular velocities of two DC motors needed are shown in Fig. 6(b). We can see that angular velocities needed are smaller when bigger friction wheels are implemented and *vice versa*. But using bigger friction wheels also mean that, a higher output torque of motor is necessary and free space available in the front of robot is reduced.

When Ψ or θ changes, which means the contact points change (r_β and h changes), the shape of the angular velocities curves also changes, as shown in Fig. 6(c). When Ψ increases, for example, from 27.9° to 35°, which means two friction wheels get closer, curves of ω_1 and ω_2 move up. When Ψ is reduced from 27.9° to 20°, curves of $\omega_1\omega_2$ sink down correspondingly. In this case, contact points shift sideways, angular velocities of two DC motors needed become smaller, but bigger torques are needed to drive

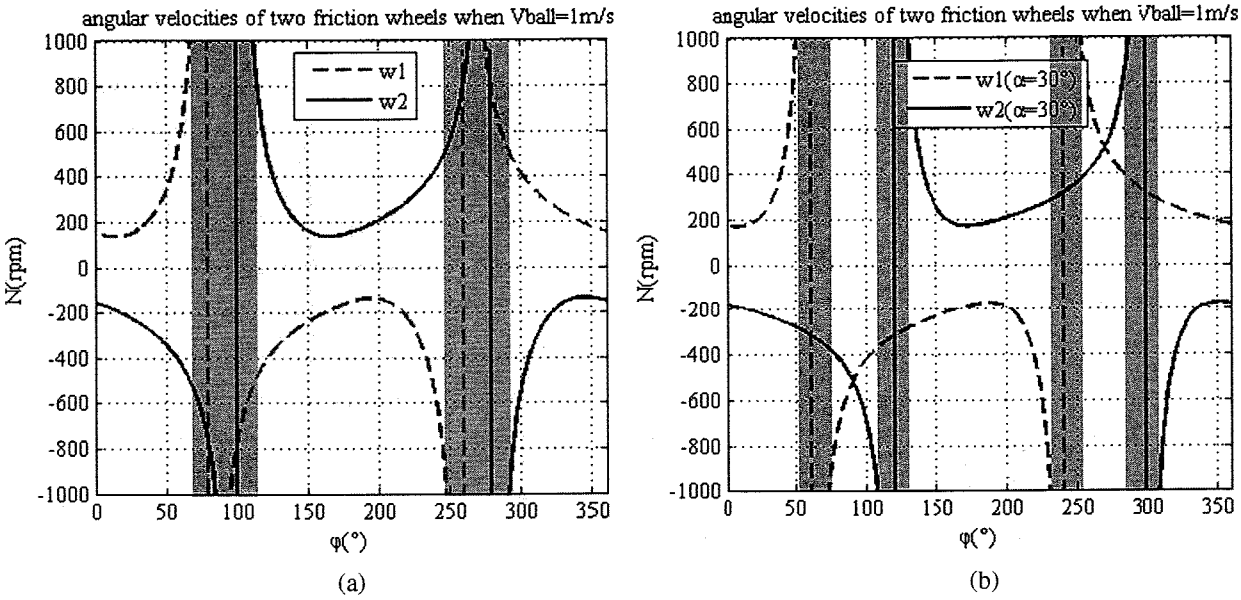

Figure 7. Angular velocities of two friction wheels needed when $V_{ball} = 1\,\text{m/s}$, $d_{wheel} = 70\,\text{mm}$, $\theta \approx 21.8°$, $\Psi \approx 27.9°$ and (a) $\alpha = 10°$, (b) $\alpha = 30°$.

the ball. Thus Ψ cannot be too small. Likewise, when α changed, for example, from 5° to 30°, the shapes of curves also changed, which is shown in Fig. 6(d). These changes are not obvious here, which will be discussed later with the help of Fig. 7.

2.4 The Control Rules of Two Wheels

We can control velocities of two wheels based on (24) and (25). Angular velocities of two wheels needed to drive the ball are shown in Fig. 7(a). Here $d_{wheel} = 70\,\text{mm}$, $\alpha = 10°$, $\theta \approx 21.8°$, $\Psi \approx 27.9°$ and the ball is driven with a velocity of 1 m/s. If $V_{ball} = 2\,\text{m/s}$, then $\omega_{1\_\text{needed}} = 2 \times \omega_1$, so is ω_2.

As we can see, when $\varphi > 67°$, ω_1 becomes very large and increases dramatically, as shown in the red rectangle area. Our DC motors cannot provide such a high speed. Thus in this case ($d_{wheel} = 70\,\text{mm}$, $\alpha = 10°$, $\theta \approx 21.8°$, $\Psi \approx 27.9°$), it is impossible for the robot to carry out lateral movement without losing the ball.

When α is changed from 10° to 30°, curves are shown in Fig. 7(b). The curve is much steeper, and the red rectangle area becomes smaller, but there are four red rectangle areas here. And with ω_1, $\omega_2 = 500\,\text{rpm}$, the robot can move laterally with the ball. If we only want to make sure that the robot can handle the ball well when dribbling forwards and backwards, the lateral movement is not important, then α should be small, from 5° to 10° is ok.

3. The Control System

The architecture of the control system of our soccer robot is shown in Fig. 8. It consists of four modules: Omni-directional vision system, Linux PC, motion controller and five motor drivers for five wheels (three on chassis and two for ball-handling). The Omni-directional vision system is in charge of self-location and ball detection. The Linux PC processes information from the Omni-directional vision system and carries out motion planning. Motion controller obtains the motion control commands from PC and controls five motors to realize the desired motion of the robot.

3.1 Cross-Coupling Control of Five Motors

There are five motors on the soccer robot, three on chassis and two for ball-handling. Three motors on chassis should accelerate or decelerate proportionally, so that the resultant velocity of the robot could increase or decrease smoothly. And the velocities of two ball-handling motors are dependent on the resultant velocity of the robot. Thus the speeds of five motors should always be in proportion or be coupled. For example, an accelerating process is shown in Fig. 9. Motor1 needs to reach a speed of 1000 rpm, while motor2 needs to get to 3000 rpm. During the acceleration, the speeds of two motors should always been maintained at a ratio of 1:3 to make sure the resultant velocity of the robot increases smoothly. Normally each motor is controlled by a PID motion controller, which is simple and effective. Each PID controller works independently. Hence, the speeds of two motors are disproportionate during acceleration, as shown in Fig. 9(a). The robot will start to move with an unexpected wriggle. Cross-coupling control of five motors is needed. In [17], a cross-coupling controller is introduced to coordinate the speeds of three motors on chassis, but it needs additional sensors to obtain the real-time linear velocity and angular velocity, based on which, the speed of each motor is adjusted to amend the resultant velocity of the robot. And it can't coordinate the speeds of two ball-handling motors with other motors. Also in [18], [20], [21] and [22], only the cross-coupling control of three chassis motors are discussed, while two ball-handling motors are not taken into consideration.

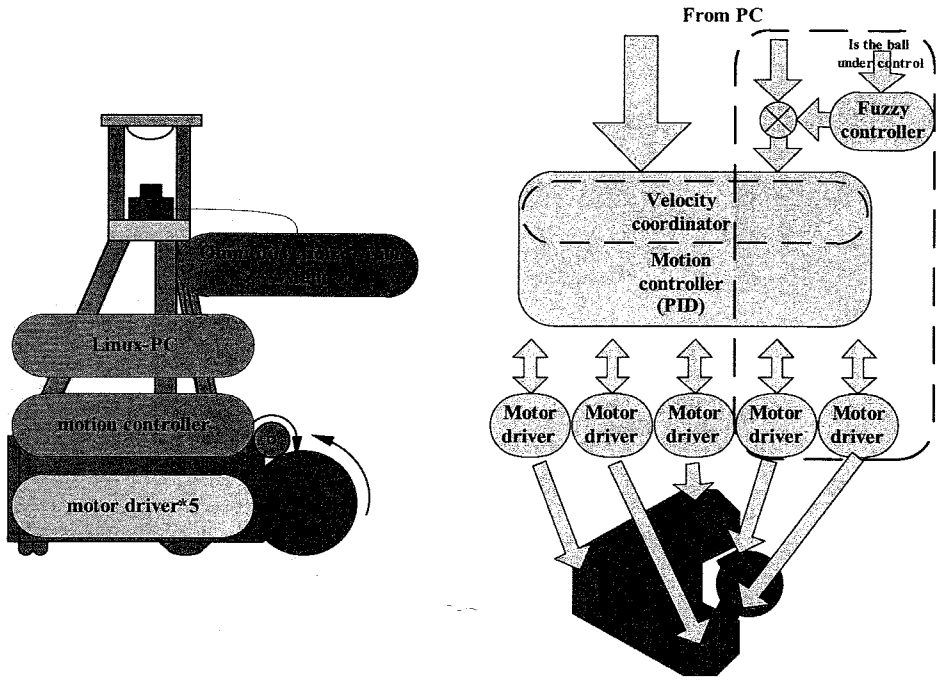

Figure 8. The architecture of the control system.

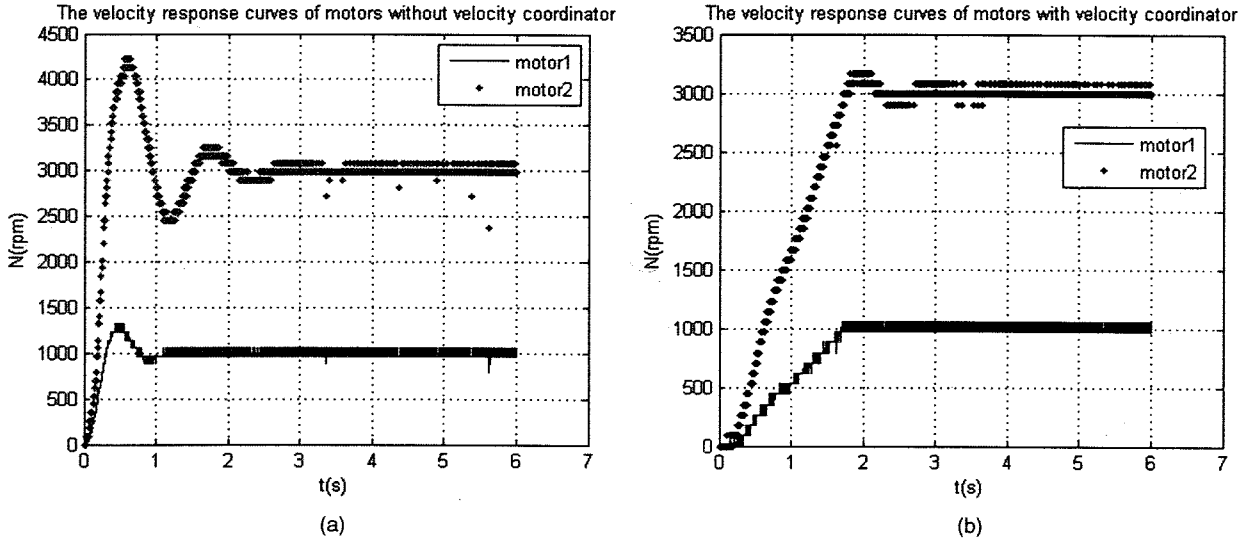

Figure 9. The acceleration process of two motors: (a) without a velocity coordinator; (b) with a velocity coordinator.

Here a velocity coordinator for five motors is added to make sure five motors accelerate or decelerate in the same pace, as shown in Fig. 8. The coordinator gets the target speeds of five motors $\{V_1, V_2, V_3, V_4, V_5\}$ from PC. Rather than control five motors directly, the coordinator will figure out at first, how long it will take for each motor to reach its target speed with the maximum acceleration of five motors.

$$\{t_1, t_2, t_3, t_4, t_5\} = \left\{ \frac{V_1}{a_{\max}}, \frac{V_2}{a_{\max}}, \frac{V_3}{a_{\max}}, \frac{V_4}{a_{\max}}, \frac{V_5}{a_{\max}} \right\}$$

$$t_{base} = \mathrm{Max}(t_1, t_2, t_3, t_4, t_5) = \frac{\mathrm{Max}(V_1, V_2, V_3, V_4, V_5)}{a_{\max}}$$

Then based on the longest acceleration time, the coordinator will adjust the accelerations of other four motors, so that five motors step up at the same pace.

$$\{a_1, a_2, a_3, a_4, a_5\} = \left\{ \frac{V_1}{t_{base}}, \frac{V_2}{t_{base}}, \frac{V_3}{t_{base}}, \frac{V_4}{t_{base}}, \frac{V_5}{t_{base}} \right\}$$

$$= \left\{ \frac{V_1 \cdot a_{\max}}{V_{\max}}, \frac{V_2 \cdot a_{\max}}{V_{\max}}, \frac{V_3 \cdot a_{\max}}{V_{\max}}, \frac{V_4 \cdot a_{\max}}{V_{\max}}, \frac{V_5 \cdot a_{\max}}{V_{\max}} \right\}$$

In this way, all motors can accelerate in the same pace, the velocity of robot increases smoothly, as shown in Fig. 9(b).

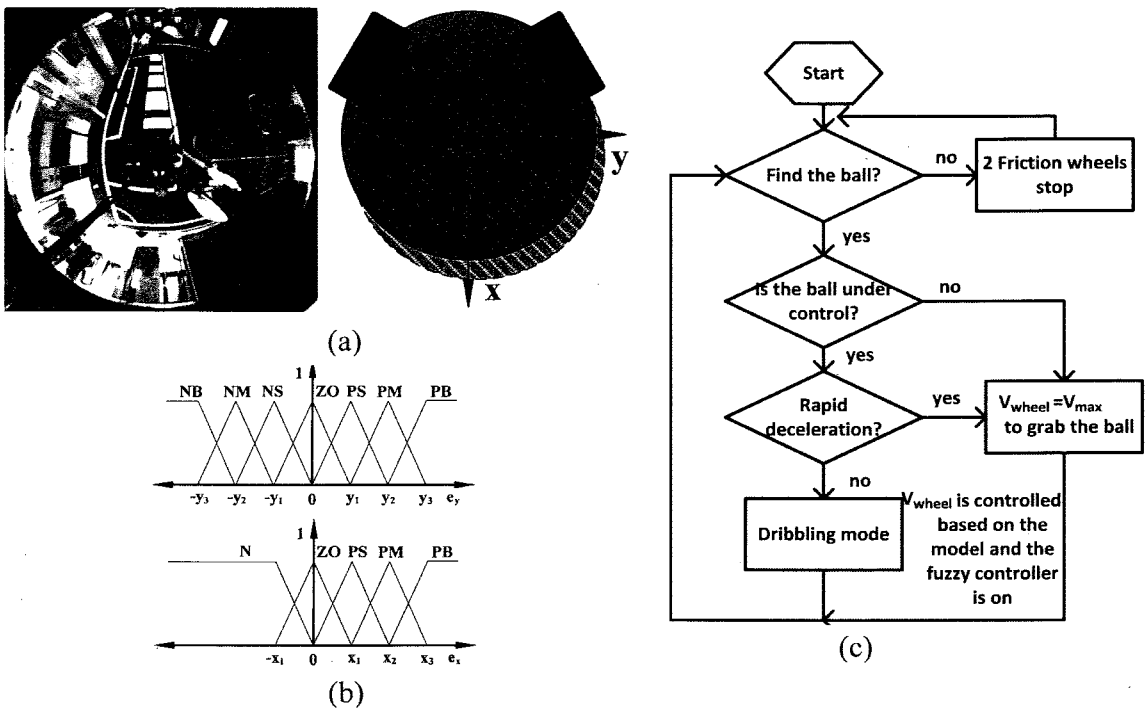

Figure 10. (a) A frame of the Omni-directional vision system. With $\Delta d = (e_x, e_y) = (x_1 - x_0, y_1 - y_0)$ as input of the fuzzy controller, velocities of two friction wheels are amended to bring the ball back to O^0_{ball}. Membership functions of input are shown in (b). The control flow chart of the ball-handling mechanism is depicted in (c).

Table 1
Rules of the Fuzzy Controller

Δn_{left} and Δn_{right}		e_y						
		NB	NM	NS	ZO	PS	PM	PB
e_x	N	PS	ZO	ZO	ZO	ZO	ZO	PS
	ZO	PS	PS	ZO	ZO	ZO	PS	PS
	PS	PM	PM	PS	PS	PS	PM	PM
	PM	PB	PB	PM	PM	PM	PB	PB
	PB	PB	PB	PB	PB	PB	PB	PB

3.2 Assisting Fuzzy Controller

In a match, the robot moves in a dynamic and oppositional environment. There are a lot of disturbances that might cause losing control of the ball. To deal with those disturbances, a feedback controller is necessary to keep the ball. Fuzzy control system is based on fuzzy logic and doesn't need the precise model of the controlled object [23]. Thus, it's very simple and effective and is widely used in the RoboCup [24], [25], [26] and [27]. In this paper, we will also utilize a fuzzy controller to help the robot protect the ball [23], [28], [29].

As shown in Fig. 10(a) is a frame from the Omni-directional vision system. When the robot is dribbling, the ball should been kept in front of the robot. Linux PC can calculate the position of the ball from this picture. When the ball is under control, the position of the ball's centre should locate at O^0_{ball}, which will be recorded. In the match, due to uncertainty of the field condition (the field may be uneven, and friction coefficient also changes in the same field), the ball's centre might be no longer in O^0_{ball}, maybe in O^1_{ball}. The distance between O^1_{ball} and O^0_{ball} can be calculated as input of the fuzzy controller. Then velocities of two friction wheels are amended to pull the ball back to O^0_{ball}. Membership functions of input are shown in Fig. 10(b). e_y ranges from $-y_2$ to y_2. In the direction of X, only positive e_x is concerned. That is because the robot can push the ball when e_x is negative. The control flow chart of the ball-handling mechanism is depicted in Fig. 10(c).

4. Experiment Results

4.1 Simulation Results

First, the model and its controller are verified with the help of a joint simulation of ADAMS and Matlab. A simplified model of ball-handling mechanism is established in ADAMS, as shown in Fig. 11. The parameters of ball-handling mechanism are given by:

$$r_{wheel} = 35\,\text{mm}; \alpha = 10^\circ; r_\beta \approx 0.64 r_{ball}; \theta \approx 27.51^\circ;$$
$$\Psi \approx 21.74^\circ; d_{ball} = 220\,\text{mm}; m_{ball} = 0.45\,\text{kg};$$

$$\mu_{dynamic}\ (\text{ball, ground}) = 0.5; \mu_{static}\ (\text{ball, ground}) = 0.7;$$
$$k_{ball} = 310\,\text{N/mm}; c = 3\ (\text{damping})$$

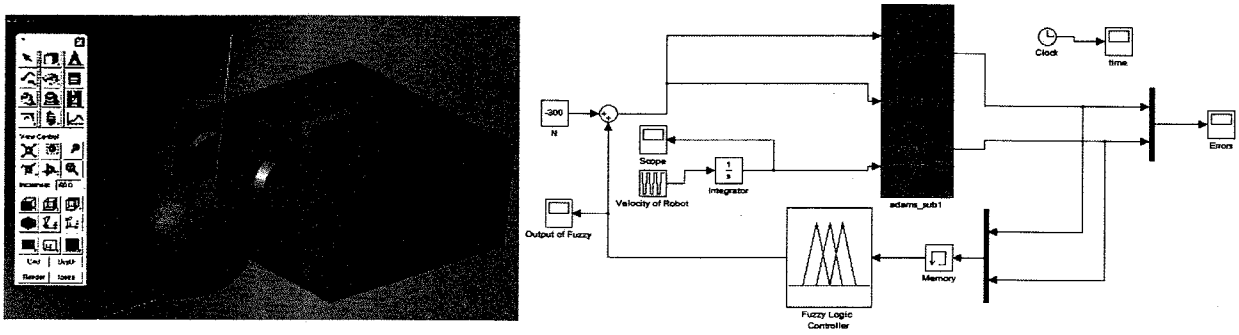

Figure 11. Simulation in ADAMS in cooperation with Matlab Simulink.

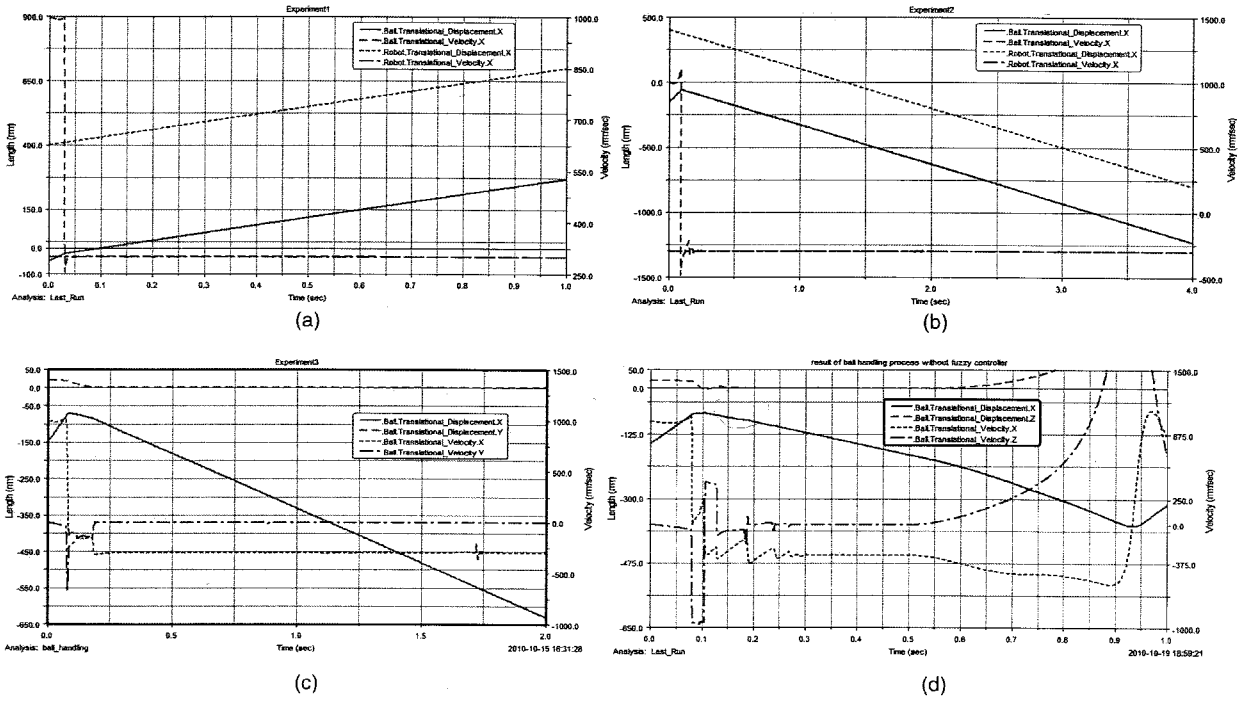

Figure 12. (a) The result of experiment 1; (b) the result of experiment 2; (c) the result of experiment 3; (d) the result of the comparison experiment of (c).

The tire model of Adams is referred to help determine those parameters for simulation.

Experiment 1: the robot moves backwards with a velocity of 300 mm/s, while the ball moves towards the robot with a velocity of 1000 mm/s.

Experiment 2: the robot moves forwards with a velocity of 300 mm/s, while the ball moves towards the robot with a velocity of 1000 mm/s.

The results are shown in Fig. 12(a) and (b). We can see that, the ball is driven with the same speed of the robot.

Experiment 3: the robot moves forwards with a velocity of 300 mm/s, while the ball moves towards the robot with a velocity of 1000 mm/s. But the initial position of the ball changes from (−150 mm, 20 mm) to (−150 mm, 0 mm), which is considered as a disturbance. The ball is no longer in the central plane of the ball-handling mechanism. The result of this experiment is shown in Fig. 12(c). The ball is taken back under control soon. The result of a comparison experiment is also shown in Fig. 12(d). In the comparison experiment, fuzzy controller is not used. When velocities of two friction wheels are not appropriate, the dribbling process will be unstable. As shown in the right figure, the ball is out of control in 0.5 s.

4.2 Hardware Experiment

Here a prototype is designed and manufactured as our test platform. Its schematic diagram is depicted in Fig. 13. The ball-handling mechanism consists of two bars. The end of each bar is mounted on the chassis of robot through a joint so that the bar can rotate around it. On the bar there is a buffer connected, as shown in Fig. 13. It is used to absorb the energy of the impact when the ball enters

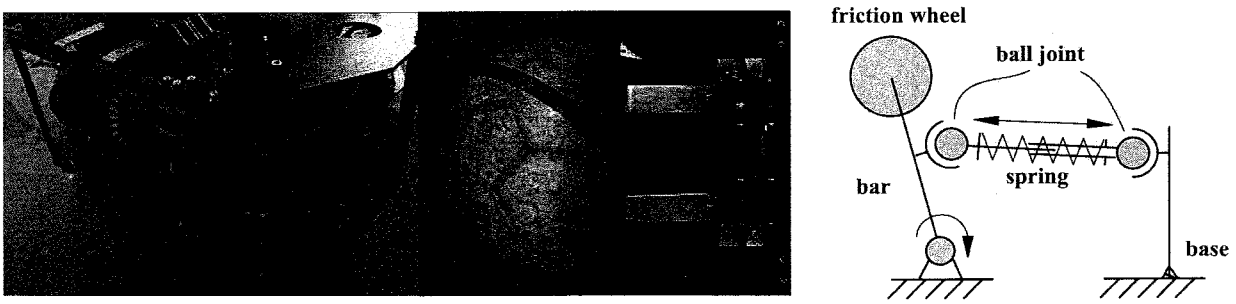

Figure 13. The active ball-handling mechanism of Jiaolong robot.

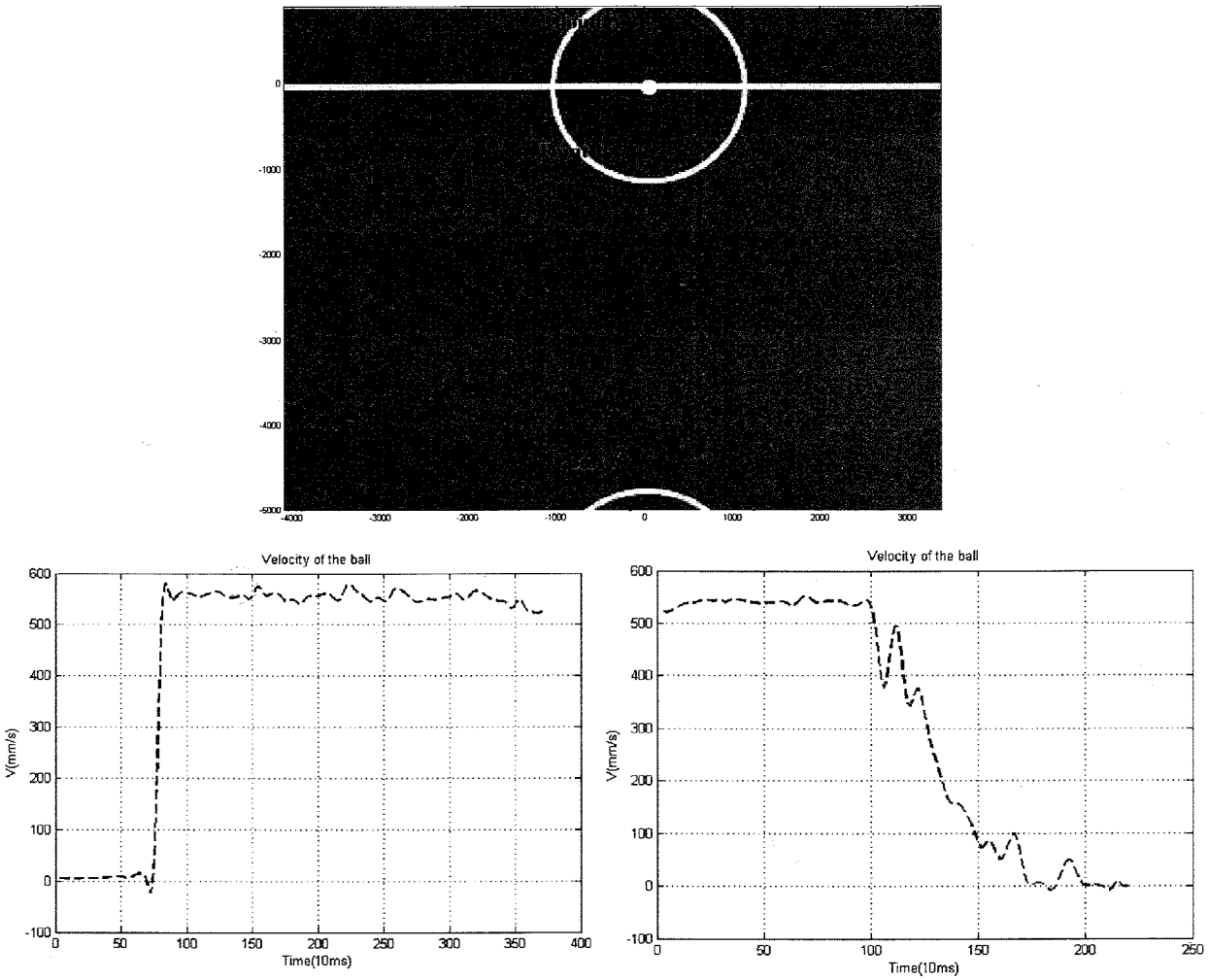

Figure 14. The result of experiment.

into the ball-handling mechanism with a high speed. Since the bar can rotate, those parameters needed in (24) and (25) are measured in the work state (when the ball is in the ball-handling mechanism), instead of in the free state. For our robot, the parameters are listed as follow:

$$r_{wheel} = 35\,\text{mm}; \alpha = 10^\circ; r_\beta \approx 0.64 r_{ball};$$
$$\theta \approx 27.51^\circ; \Psi \approx 21.74^\circ$$

Experiment: The initial position of robot is Point A and the ball locates at Point B at first. The robot finds and catches the ball, then dribbles the ball from Point B to Point C and stops at Point C, as shown in Fig. 14. Velocity of the ball is shown in the figure below. Velocity is calculated by differentiating the position data. A filter is used to process those velocity data to make the curve smooth. The bottom left picture shows the velocity of the ball when the robot dribbles forwards. The bottom right picture shows the velocity of the ball when the robot decelerates. When the robot decelerates, the ball's momentum still carries it forwards. The compressed spring (as shown in Fig. 13) is released. Thanks to that,

the friction wheels can still touch and exert forces on the ball. Then the fuzzy controller adjusts the velocities of two wheels to pull the ball back. Thus, the ball will decelerate gradually. Finally, the robot stops with the ball. While in the acceleration process, the ball can also be pushed forwards since the spring is compressed. The ball will accelerate to the speed of the robot quickly. That's why the velocity control performance of acceleration is better than deceleration.

5. Conclusion and Future Work

In this paper, an active ball-handling mechanism for soccer robot in RoboCup is designed and utilized in the MSL team Shanghai Jiaolong. The ball-handling mechanism consists of two friction wheels and the ball-handling process is performed by individual control of two friction wheels' rotation velocities. Compared to other methods proposed for active ball-handling, this method is simple and effective. A theoretical model of such kind of active ball-handing mechanism is derived, and effects caused by different ways of installation and different installation parameters are analyzed. Two DC motors' rotation velocities can be directly obtained according to Fig. 7, which can be turned into a table stored in the Linux PC. A velocity coordinator is then devised to optimize the motion of robot. In addition, a fuzzy controller adjusts velocities of two DC motors based on the ball's position obtained from the Omni-directional vision system, so as to make sure the ball is always under control. The design of fuzzy controller is not complicated and better results can be achieved by refinement of the fuzzy control rules. In the end of this paper, a joint simulation of Matlab and Adams was utilized to help design the fuzzy controller. And some experiments were carried out to verify the effectiveness of this method. The result shows that, the robot can handle the ball well.

But in practice, we find that, the position of the ball obtained from the Omni-directional vision system is not stable despite a filter is used to process those position data. This may be caused by many factors. For example, omnidirectional wheels are used in the soccer robot, which cause vibration during the movement. The body of the robot shakes a lot. So does the body of camera. And the ball's position obtained from the Omni-directional vision system is also effected by the ambient light. Due to those reasons, the effect of the fuzzy controller is weakened. We have to find another way to help determining the precise position of the ball in the future. Only with precise real-time positions, the fuzzy controller can adjust the control precisely, so as to improve the robustness of the control system. Further information about our works are presented on our website http://robolab.sjtu.edu.cn/robocup/

Acknowledgement

This paper is supported by Doctoral Fund of Ministry of Education of China (No. 20090073110037) and the Research Fund of State Key Lab of MSV, China (No. MSV201101). We would like to thank Shanghai Ingenious Automation Technology for helping us design and manufacture the new Jiaolong soccer robot. Also, we extend our thanks to Xiaoxiao Zhu for his help in the experiments.

References

[1] Rules and Regulations of RoboCup, RoboCup 2010 official site, http://www.robocup2010.org (accessed December 14, 2010).

[2] S. Stancliff, Evolution of active dribbling mechanisms in RoboCup, 16-741 Project, April 25, 2005, http://citeseerx.ist.psu.edu/viewdoc/download?doi=10.1.1.87.2173&rep=rep1&type=pdf (accessed December 14, 2010).

[3] R. D'Andrea, T. Kalmar-Nagy, P. Ganguly, and M. Babish, The Cornell Robocup team, in P. Stone, T. Balch, and G. Kraetzschmar (Eds.) *RoboCup 2000: Robot Soccer World Cup IV* (New York, NY: Springer, 2002), 41–51.

[4] D. Chung, A. Dhanaliwala, S. Kim, J. Leou, E. Malone, J. Miller, E. Nice, S. Richardson, and K. Sterk, RoboCup Mechanical Engineering Documentation Fall 2001–Spring 2002, http://www.cis.cornell.edu/boom/2005/ProjectArchive/robocup/documentation.php (accessed December 14, 2010).

[5] Team CAMBADA, CAMBADA'2010: Team Description Paper, RoboCup2010, Singapore, www.ieeta.pt/atri/cambada/docs/CAMBADA-tdp-2010.pdf (accessed December 14, 2010).

[6] Team FU Fighter, Team Description FU Fighter 2005, RoboCup2005, Osaka, Japan, http://robocup.mi.fu-berlin.de/pmwiki/Main/Publications (accessed December 14, 2010).

[7] Team Tech United Eindhoven, Tech United Eindhoven Team Description 2010, RoboCup2010, Singapore, www.techunited.nl/media/files/team_description_paper_2010.pdf (accessed December 14, 2010).

[8] Team ENDEAVOR, ENDEAVOR Team Description Paper 2010, RoboCup2010, Singapore, http://elc.wzvtc.net.cn/robot/img/ENDEAVOR%20Team%20Description%20Paper%202010-2010-2-10-2.pdf (accessed December 14, 2010).

[9] Team NuBot, NuBot Team Description Paper 2010, RoboCup-2010, Singapore, http://www.nubot.com.cn/teamDsc/NuBot%20TDP%202010.pdf (accessed December 14, 2010).

[10] Team Water, Water Team Description Paper 2010, RoboCup-2010, Singapore, http://jdgcxy.bistu.edu.cn/robocup/file/description/Team%20Description%20PaperInnovations%20of%20the%20team.pdf (accessed December 14, 2010).

[11] G. Stefan, A. Harald, B. Bernd, H. Alexander, H. Christof, J. Thomas, M. Thomas, M. Michael, M.K. Stephan, M. Daniel, P. Christopher, S. Gerald, U. Robert, and W. Franz, Mostly harmless: Team description paper 2009, *RoboCup International Symposium*, Graz, Austria, 2009.

[12] T. Hoshi and H. Shinoda, Robot skin based on touch-are-sensitive tactile element, *Proceedings of the 2006 IEEE International Conference on Robotics and Automation (ICRA2006)*, Orlando, FL, 2006, 3463–3468.

[13] R. Hoogendijk, *Design of a ball-handling mechanism for Robocup*, Bachelor End Project, Technische Universiteit Eindhoven, Eindhoven, Niederlande, 2007.

[14] S. Lu, D. Hai, X. Wang, F. Sun, and Z. Zheng, Design of the active ball-handling mechanism of RoboCup MSL robot, *Mechanical and Electrical Engineering Magazine, 26*(11), 2009, 13–17.

[15] J. De Best, R. van de Molengraft, and M. Steinbuch, A novel ball-handling mechanism for the RoboCup middle size league, *Mechatronics, 21*, 2011, 469–478.

[16] J. De Best and R. van de Molengraft, An active ball-handling mechanism for RoboCup, *International Conference on Control, Automation, Robotics and Vision 2008* (ICARCV2008), Hanoi, 2060–2065.

[17] D. Shen and Q. Cao, Multi-axis coordinated motion of three-wheel omni-directional mobile robot based on speed cross-coupling control, *Journal of Mechanical and Electrical Engineering, 16*(1), 2010, 50–52.

[18] M. Sherback, O. Purwin, and R. D'Andrea, Real-time motion planning and control in the 2005 Cornell RoboCup system, *Lecture Notes in Control and Information Sciences, 335*, 2006, 245–263.

[19] H. Altinger, S.J. Galler, S. Muehlbacher-Karrer, G. Steinbauer, F. Wotawa, and H. Zangl, Concept evaluation of a reflex inspired ball-handling device for autonomous soccer robots, in J. Baltes, M.G. Lagoudakis, T. Naruse, and S. Shiry (Eds.), *RoboCup 2009: Robot Soccer World Cup XIII, Lecture notes in computer science, 5949* (New York, NY: Springer, 2010), 11–22.

[20] B. Carter, M. Good, M. Dorohoff, J. Lew, R.L. Williams II, and P. Gallina, Mechanical design and modeling of an omnidirectional RoboCup player, *Proceedings of Fifth RoboCup 2001 International Symposium*, Citeseer, Seattle, WA, 2001, 1–6.

[21] M. Schulé, M. Schanz, H. Felger, R. Lafrenz, P. Levi, and J. Starke, Control of autonomous robots in the RoboCup scenario using coupled selection equations, *Tagungsband des 17. Fachgesprächs Autonome Mobile Systeme 2001(AMS2001)*, Stuttgart, Deutschland, 2001, 57–63.

[22] T.K. Nagy, R. D'Andrea, and P. Ganguly, Near-optimal dynamic trajectory generation and control of an omnidirectional vehicle, *Robotics and Autonomous Systems, 46*(1), 2004, 47–64.

[23] J. Jantzen, *Design of fuzzy controllers*, Technical Report No. 98-E864, Department of Automation, Technical University of Denmark, http://www.iau.dtu.dk/~jj/pubs/design.pdf (accessed December 14, 2010).

[24] A. Bonarini, G. Invernizzi, T.H. Labella, and M. Matteucci, An architecture to coordinate fuzzy behaviors to control an autonomous robot, *Fuzzy Sets and Systems, 134*(1), 2003, 101–115.

[25] A. Saffiotti and Z. Wasik, Using hierarchical fuzzy behaviors in the RoboCup domain, *Autonomous Robotic Systems, 116*, 2003, 235–262.

[26] V. Rostami, O. Sojodishijani, S. Ebrahimijam, and A. Mohseni, Fuzzy error recovery in feedback control for three wheel omnidirectional soccer robot, *International Conference in Enformatika System Science and Engineering*, Istanbul, Turkey, *9*, 2005, 91–94.

[27] B. Innocenti, B. Lópeza, and J. Salvia, A multi-agent architecture with cooperative fuzzy control for a mobile robot, *Robotics and Autonomous Systems, 55*(12), 2007, 881–891.

[28] Kevin M. Passino and Stephen Yurkovich, *Fuzzy control*, 1st ed. (Upper Saddle River, NJ: Addison-Wesley Longman Inc., 1998).

[29] J. Klir, Ute St. Clair, and Bo Yuan, *Fuzzy set theory: Foundations and applications*, 1st ed. (Upper Saddle River, NJ: Prentice Hall, 1997).

[30] Javier Ruiz-del Solar, Eric Chown and Paul G. Ploeger, *RoboCup 2010: Robot Soccer World Cup XIV*, 1st ed. (Berlin: Springer, 2010).

Biographies

Aolin Tang received his B.Eng. and M.Eng. degrees in 2008 and 2010, respectively, from Tong Ji University and Shanghai Jiao Tong University. He is currently working toward the Ph.D. degree in the State Key Lab of Mechanical Systems and Vibration at the Shanghai Jiao Tong University, Shanghai, China and his research interests include motion control, mobile robot, surgical robot and home service robot.

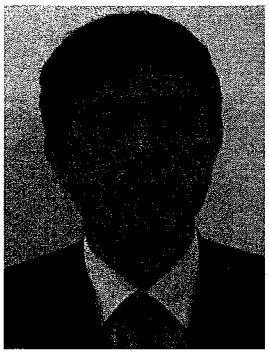

Qixin Cao received the M.Eng. and Ph.D. in 1994 and 1997, respectively, from Miyazaki University and Kagoshima University. He is currently the vice president of the research institute of robotics in the Shanghai Jiao Tong University. His research interests include machine vision, pattern recognition, intelligent robot, modular technology of robot, intelligent maintenance and internet of things.

Chunshan Xu is currently the manager of Shanghai Ingenious Automation Technology Co., Ltd.